

---

# Princeton Plasma Physics Laboratory

---

PPPL-

PPPL-



Prepared for the U.S. Department of Energy under Contract DE-AC02-09CH11466.

# Princeton Plasma Physics Laboratory

## Report Disclaimers

---

### Full Legal Disclaimer

This report was prepared as an account of work sponsored by an agency of the United States Government. Neither the United States Government nor any agency thereof, nor any of their employees, nor any of their contractors, subcontractors or their employees, makes any warranty, express or implied, or assumes any legal liability or responsibility for the accuracy, completeness, or any third party's use or the results of such use of any information, apparatus, product, or process disclosed, or represents that its use would not infringe privately owned rights. Reference herein to any specific commercial product, process, or service by trade name, trademark, manufacturer, or otherwise, does not necessarily constitute or imply its endorsement, recommendation, or favoring by the United States Government or any agency thereof or its contractors or subcontractors. The views and opinions of authors expressed herein do not necessarily state or reflect those of the United States Government or any agency thereof.

### Trademark Disclaimer

Reference herein to any specific commercial product, process, or service by trade name, trademark, manufacturer, or otherwise, does not necessarily constitute or imply its endorsement, recommendation, or favoring by the United States Government or any agency thereof or its contractors or subcontractors.

---

## PPPL Report Availability

### Princeton Plasma Physics Laboratory:

<http://www.pppl.gov/techreports.cfm>

### Office of Scientific and Technical Information (OSTI):

<http://www.osti.gov/bridge>

---

### Related Links:

[U.S. Department of Energy](#)

[Office of Scientific and Technical Information](#)

[Fusion Links](#)

# Two-stream stability properties of the return-current layer for intense ion beam propagation through background plasma

Edward A. Startsev, Ronald C. Davidson and Mikhail Dorf

Plasma Physics Laboratory, Princeton University, Princeton, New Jersey 08543

When an ion beam with sharp edge propagates through a background plasma, its current is neutralized by the plasma return current everywhere except at the beam edge over a characteristic transverse distance  $\Delta x_{\perp} \sim \delta_{pe}$ , where  $\delta_{pe} = c/\omega_{pe}$  is the collisionless skin depth, and  $\omega_{pe}$  is the electron plasma frequency. Because the background plasma electrons neutralizing the ion beam current inside the beam are streaming relative to the background plasma electrons outside the beam, the background plasma can support a two-stream surface-mode excitation. Such surface modes have been studied previously assuming complete charge and current neutralization, and have been shown to be strongly unstable. In this paper we study the detailed stability properties of this two-stream surface mode for an electron flow velocity profile self-consistently driven by the ion beam. In particular, it is shown that the self-magnetic field generated inside the unneutralized current layer, which has not been taken into account previously, completely eliminates the instability.

## I. INTRODUCTION

Ion beam propagation in neutralizing background plasma is of interest for many applications, including ion-beam-driven high energy density physics and heavy ion fusion. The background plasma is needed to neutralize the ion beam space charge and beam current so that it can be transported and efficiently focused either ballistically or by the remnant unneutralized self-magnetic field or applied magnetic field [1–4]. The ion beam current is neutralized by the opposing background plasma electron return current [5–7], which implies that the plasma electrons inside the beam flow with average velocity  $v_{e0} = Z_b(n_b/n_{e0})v_b$  relative to the electrons outside of the beam. Here  $v_b$  is the beam velocity,  $Z_b$  is the beam charge state, and  $n_b$  and  $n_{e0}$  are the beam density and background electron densities, respectively. One of the main disadvantages of using plasma to transport and focus intense ion beams is that the ion beam propagation in background plasma may be subject to collective instabilities. There is a growing body of literature dedicated to studying collective beam-plasma interactions. For a recent review of collective beam-plasma instabilities see Ref. [8]. One of the fastest instabilities involving the lightest species is the two-stream instability between the electrons flowing inside the beam and the stationary electrons outside the beam. Such

an instability has been studied previously by several authors and has been shown to have maximum growth rate of the order of the background electron plasma frequency  $\omega_{pe} = (4\pi e^2 n_{e0}/m_e)^{1/2}$  [8–10]. Here  $-e$  is the electron charge and  $m_e$  is the electron mass. The usual assumption made in the analysis of this fast two-stream instability is that the beam density has a sharp transverse profile, with constant density  $n_b$  inside the beam, and zero density beyond a certain radius  $r_b$ . It is also assumed that the beam current is completely neutralized by the return electron current flowing inside the beam [8, 9]. It had been shown for such a charge-current distribution that there exists an unstable low-frequency electrostatic mode propagating along the beam direction which is localized near the beam edge. It follows from Poisson’s equation that for the mode with the longitudinal wavenumber  $k_z$ , the transverse wavenumber  $k_\perp$  satisfies the equation

$$k_\perp^2 = -k_z^2 < 0, \quad (1)$$

which implies that  $k_\perp$  is pure imaginary, and therefore, the mode electric field approaches zero exponentially away from the beam edge. In the case where  $k_z^2 r_b^2 \gg 1$ , the approximate dispersion relation is given by [8, 9]

$$\left[ 1 - \frac{\omega_{pe}^2}{\omega^2} \right] + \left[ 1 - \frac{\omega_{pe}^2}{(\omega - k_z v_{e0})^2} \right] = 0. \quad (2)$$

When  $q^2 = (2\omega_{pe}/k_z v_{e0})^2 > 1$ , Eq. (2) has an unstable solution  $\omega$  with maximum growth rate  $(Im\omega)_{max} = \gamma_{max} = \omega_{pe}/2$ . For  $q^2 \ll 1$  the unstable solution is given approximately by

$$\omega = \frac{k_z v_{e0}}{2} + i \frac{|k_z| v_{e0}}{2}. \quad (3)$$

Here and in what follows, we assume that  $v_{e0}$  is positive ( $v_{e0} > 0$ ). If such an instability exists, it would lead to strong heating of the background electrons and also to the excitation of large-amplitude plasma oscillations which could result in a significant deterioration of the beam quality, which would be very undesirable for most beam physics applications. In this paper we reconsider the derivation of Eq. (2) without assuming full beam current neutralization. Indeed, for an ion beam propagating through neutralizing background plasma, the electron flow velocity changes over a layer of characteristic transverse width  $\delta_\perp \sim \delta_{pe} \equiv c/\omega_{pe}$  [5–7]. For finite layer width  $\delta_\perp$ , the growth rate of a mode with transverse wavelength  $k_\perp$  is reduced according to  $\gamma(k_\perp) = \gamma(|k_\perp| \sim 1/\delta_\perp) \times \exp(-|k_\perp| \delta_\perp)$ . Therefore, for a layer with width  $\delta_\perp \sim \delta_{pe}$ , the maximum growth rate is for  $|k_z| \sim 1/\delta_{pe}$ , which corresponds to

$$\gamma_{max} \sim |\omega| \sim |k_z| v_{e0} \sim \left( \frac{v_{e0}}{c} \right) \omega_{pe}. \quad (4)$$

One the other hand, the unneutralized current in the layer also creates a transverse self-magnetic field  $B_0$ . Since for long beams with length  $L_b \gg v_b/\omega_{pe}$  the electron longitudinal canonical momentum  $p_{e0}$  remains approximately zero [7], the electron cyclotron frequency  $\omega_{ce} = eB_0/m_e c$  inside the layer is given approximately by  $p_{e0} = m_e v_{e0} - \frac{eA_0}{c} = 0$ , which implies

$$\omega_{ce} = \frac{dv_{e0}}{dx_{\perp}} \approx \left(\frac{v_{e0}}{c}\right) \omega_{pe}. \quad (5)$$

Since  $|\omega| \sim \gamma_{max} \sim \omega_{ce}$ , this mode is strongly affected by the self-magnetic field. In the detailed analysis that follows in this paper, we will compare the dispersion relation that includes the self-magnetic field in the layer with the dispersion relation where it is omitted. The detailed analysis shows that the self-magnetic field completely eliminates the fast two-stream instability.

The organization of this paper is the following. In Sec. II, the steady-state neutralization of the ion beam current by the background plasma electrons is reviewed. In Sec. III, the linearized equations governing the collective dynamics of the background plasma electrons and the associated electromagnetic excitations are derived. In Sec. IV, the linearized equations are analyzed in detail both analytically and numerically, and it is shown that the inclusion of self-magnetic field effects completely eliminates the fast two-stream instability. Finally, the conclusions are summarized in Sec. V.

## II. RETURN CURRENT FLOW VELOCITY DISTRIBUTION

The analysis presented in this paper is carried out for nonrelativistic ion beams with  $v_b^2/c^2 \ll 1$ . To simplify the analysis, we assume that the transverse ion beam dimension is large enough so that for modes localized near the beam edge a 2D planar approximation is valid, or that  $k_{\perp}^2 r_b^2 \gg 1$ , where  $r_b$  is the beam radius and  $k_{\perp}$  is the characteristic wavenumber transverse to the beam propagation direction. We assume that the beam propagates along the  $z$ -axis (longitudinal direction) with average velocity  $v_b$ . The neutralizing electron current also flows in  $z$ -direction with average velocity  $v_{e0}(y)$ , which is a function of the transverse coordinate  $y$  (radial direction) (Fig. 1).

As the ion beam propagates through the background plasma, the changing magnetic field in the unneutralized beam head generates a longitudinal electric field which accelerates the background electrons to velocity  $v_{e0}(y)$ . From the conservation of electron longitudinal canonical momentum  $p_{e0} = m_e v_{e0} - eA_0/c$  for a long ion beam with  $L_b \gg v_b/\omega_{pe}$ , it follows that

$$v_{e0}(y) = \frac{eA_0(y)}{m_e c} \quad \text{or} \quad \frac{d}{dy} v_{e0} = \omega_{ce}(y), \quad (6)$$

where  $A_0$  is the vector potential,  $B_0 = dA_0/dy$  is the self-magnetic field (in the  $x$ -direction, see Fig. 1), and  $\omega_{ce} = eB_0/m_e c$  is the electron cyclotron frequency.

The longitudinal current density  $j_z = -e(n_{e0}v_{e0} - Z_b n_b v_b)$  generates the self-magnetic field  $B_0$  according to

$$\frac{d}{dy}B_0 = \frac{4\pi}{c}e[n_{e0}v_{e0} - Z_b n_b v_b], \quad \text{or equivalently, } \frac{d}{dy}\omega_{ce} = \left(\frac{\omega_{pe}}{c}\right)^2 \left[ v_{e0} - Z_b \left(\frac{n_b}{n_{e0}}\right) v_b \right]. \quad (7)$$

For a long ion beam with  $L_b \gg v_b/\omega_{pe}$ , quasi-neutrality is a very good approximation

$$n_{e0}(y) = Z_b n_b(y) + n_0, \quad (8)$$

where  $n_0$  is the background ion density, and we have assumed that the background plasma ions are singly ionized. From Eqs. (6)–(8), we obtain the equation for the flow velocity of the background electrons

$$\left[ \delta_{pe}^2 \frac{d^2}{dy^2} - 1 \right] v_{e0}(y) = -Z_b \left(\frac{n_b}{n_{e0}}\right) v_b. \quad (9)$$

Here,  $\delta_{pe} = c/\omega_{pe}$  is the electron skin depth.

For a beam with small density  $Z_b n_b \ll n_0$ , which is constant out to the beam edge at  $y = 0$ , it follows from Eq. (9) that the beam current is unneutralized over a characteristic distance  $\delta_{pe}$  near the beam edge, and the electron velocity profile is given by

$$v_{e0}(y) = \frac{v_b}{2} \frac{Z_b n_b}{n_0} \times \begin{cases} [2 - \exp(-y/\delta_{pe})], & y > 0, \\ \exp(y/\delta_{pe}), & y < 0. \end{cases} \quad (10)$$

The electron velocity profile [Eq. (10)] is illustrated in Fig. 2. The self-magnetic field exists within a layer of width  $\delta_{pe}$  near the beam edge at  $y = 0$ , with profile given by

$$\frac{eB_0}{m_e c} \equiv \omega_{ce}(y) = \frac{d}{dy}v_{e0} = \frac{v_b}{2\delta_{pe}} \frac{Z_b n_b}{n_0} \exp(-|y|/\delta_{pe}). \quad (11)$$

In addition to the self-magnetic field [Eq. (11)], there also exists a transverse self-electric field  $E_0$  (in the  $y$ -direction) which is needed to balance the magnetic part of the Lorentz force acting on an electron fluid element in steady state. It is readily shown that

$$\frac{e}{m_e} E_0 = -v_{e0} \frac{e}{m_e c} B_0 = -\frac{d}{dy}v_{e0}^2. \quad (12)$$

The degree of the departure from quasi-neutrality [Eq. (8)] can be obtained from Poisson's equation, and Eqs. (10) and (12). We obtain

$$\frac{\delta n_{e0}}{Z_b n_b} = -\frac{1}{4\pi e Z_b n_b} \frac{d}{dy} E_0 = \frac{n_0}{Z_b n_b} \delta_{pe}^2 \frac{d^2}{dy^2} \left( \frac{v_{e0}^2}{c^2} \right) \sim \frac{Z_b n_b}{n_0} \beta_b^2, \quad (13)$$

where  $\beta_b = v_b/c$ . For a nonrelativistic ion beam with  $\beta_b^2 \ll 1$ , the departure from quasi-neutrality is extremely small, and will be neglected [7] in the subsequent analysis.

### III. LINEARIZED EQUATIONS FOR BACKGROUND PLASMA ELECTRONS

In this section, we derive the linearized equations governing the collective dynamics of the background plasma electrons and the associated electromagnetic excitations about the equilibrium profiles described in the previous section. In the analysis it is assumed that the characteristic mode frequencies are much larger than the beam and background ion plasma frequencies,  $|\omega| \gg \omega_{pb}, \omega_{pi}$ , and therefore the motion of the beam ions and plasma ions are neglected. Here  $\omega_{ps}^2 = 4\pi e^2 Z_s^2 n_s / m_s$ , and  $s = i, b$ . We also consider here only excitations with zero azimuthal component of electric field  $E_x = 0$ .

The equation for the perturbed electric field  $\mathbf{E}$  can be obtained by combining the time derivative of the  $\nabla \times \mathbf{B}$  Maxwell equation with the curl of the  $\nabla \times \mathbf{E}$  Maxwell equation to give

$$\left( \frac{1}{c^2} \frac{\partial^2}{\partial t^2} - \nabla^2 \right) \mathbf{E} + \nabla(\nabla \cdot \mathbf{E}) = -\frac{4\pi}{c^2} \frac{\partial \mathbf{j}}{\partial t}. \quad (14)$$

Here, the perturbed current is given by  $\mathbf{j} = -e(n_0 \mathbf{v} + n v_{e0} \mathbf{e}_z)$ , where  $n$  and  $\mathbf{v}$  are the perturbed electron density and flow velocity, respectively. We express perturbed quantities as  $\Psi(y, z, t) = \Psi(y) \exp(ik_z z - i\omega t)$ , where  $Im\omega > 0$  corresponds to instability (temporal growth). The perturbed current in Eq. (14) can be determined from the linearized electron continuity equation

$$-i[\omega - k_z v_{e0}(y)]n + ik_z(n_0 v_z) + \frac{d}{dy}(n_{e0} v_y) = 0, \quad (15)$$

and the linearized electron momentum equations

$$\begin{aligned} -i[\omega - k_z v_{e0}(y)]v_y + \omega_{ce} v_z &= -\left(\frac{e}{m_e}\right) \left(E_y + \frac{v_{e0}}{c} B_x\right), \\ -i[\omega - k_z v_{e0}(y)]v_z + v_y \frac{d}{dy} v_{e0} - \omega_{ce} v_y &= -\left(\frac{e}{m_e}\right) E_z, \end{aligned} \quad (16)$$

where  $\omega_{ce} = eB_0/mc$  is given by Eq. (11). Furthermore, the perturbed magnetic field  $B_x$  can be expressed in terms of electric field components  $E_z$  and  $E_y$  as

$$i\omega B_x = \frac{d}{dy} E_z - ik_z E_y \quad (17)$$

Using  $\omega_{ce} = dv_{e0}/dy$ , and combining Eqs. (14)–(17) we obtain two coupled equations for electric field components  $E_y$  and  $E_z$ , i.e.,

$$\left(k_z^2 - \frac{\omega^2}{c^2}\right) E_y + ik_z \frac{d}{dy} E_z = -k_{pe}^2 \left[ E_y - i \frac{d}{dy} \left( \frac{v_{e0} E_z}{\omega - k_z v_{e0}} \right) \right], \quad (18)$$

$$\begin{aligned} -\left(\frac{d^2}{dy^2} + \frac{\omega^2}{c^2}\right) E_z + ik_z \frac{d}{dy} E_y &= -k_{pe}^2 \frac{\omega^2}{(\omega - k_z v_{e0})^2} E_z \\ &+ i \frac{v_{e0}}{\omega - k_z v_{e0}} \frac{d}{dy} \left\{ k_{pe}^2 \left[ E_y - i \frac{d}{dy} \left( \frac{v_{e0} E_z}{\omega - k_z v_{e0}} \right) \right] \right\}. \end{aligned} \quad (19)$$

Here  $k_{pe}^2 = \omega_{pe}^2/c^2$ . Eliminating the  $E_y$  component using Eq. (18), we obtain the equation for the  $E_z$  component

$$\begin{aligned} \frac{d}{dy} \left[ \frac{1}{(k_z^2 + k_{pe}^2 - \omega^2/c^2)} \frac{d}{dy} E_z \right] - \frac{1}{(\omega - k_z v_{e0})} \frac{d}{dy} \left\{ \frac{\omega_{pe}^2}{(k_z^2 + k_{pe}^2 - \omega^2/c^2)} \frac{d}{dy} \left[ \frac{E_z}{(\omega - k_z v_{e0})} \right] \right\} \\ = \left[ 1 - \frac{\omega_{pe}^2}{(\omega - k_z v_{e0})^2} \right] E_z. \end{aligned} \quad (20)$$

In deriving Eq. (20) we used the approximation  $v_{e0}^2/c^2 \ll 1$ .

If the equilibrium self-magnetic field is neglected ( $\omega_{ce} = 0$ ), the two equations for the electric field components  $E_y$  and  $E_z$  become

$$\left( k_z^2 - \frac{\omega^2}{c^2} \right) E_y + ik_z \frac{d}{dy} E_z = -k_{pe}^2 \left[ E_y - i \left( \frac{v_{e0}}{\omega - k_z v_{e0}} \right) \frac{d}{dy} E_z \right], \quad (21)$$

$$\begin{aligned} - \left( \frac{d^2}{dy^2} + \frac{\omega^2}{c^2} \right) E_z + ik_z \frac{d}{dy} E_y = -k_{pe}^2 \frac{\omega^2}{(\omega - k_z v_{e0})^2} E_z \\ + i \frac{d}{dy} \left\{ \frac{v_{e0} k_{pe}^2}{\omega - k_z v_{e0}} \left[ E_y - i \left( \frac{v_{e0}}{\omega - k_z v_{e0}} \right) \frac{d}{dy} E_z \right] \right\}. \end{aligned} \quad (22)$$

Eliminating the  $E_y$  component using Eq. (21), we obtain the equation for the  $E_z$  component

$$\frac{d}{dy} \left\{ \frac{1}{(k_z^2 + k_{pe}^2 - \omega^2/c^2)} \left[ 1 - \frac{\omega_{pe}^2}{(\omega - k_z v_{e0})^2} \right] \frac{d}{dy} E_z \right\} = \left[ 1 - \frac{\omega_{pe}^2}{(\omega - k_z v_{e0})^2} \right] E_z. \quad (23)$$

Note that in the electrostatic limit with  $k_z^2 \gg |k_{pe}^2 - \omega^2/c^2|$ , Eq. (23) reduces to the equation previously derived in Refs. [8, 9], whereas Eq. (20) does not. This is because even in this limit the effects of the self-magnetic field are *not* negligibly small!

#### IV. ANALYSIS OF THE LINEARIZED EQUATION

Equations (20) and (23) were derived using a Fourier transform of the linearized equations. Below we are interested in the solution to the initial-value problem which requires a Laplace transform with respect to time  $t$ . The difference between using Fourier and Laplace transforms is the presence of source terms on the right-hand side of Eqs. (20) and (23) which are related to the initial conditions for  $E_z \equiv E$  and its derivatives at time  $t = 0$ .

The solution to the initial-value problem for Eq. (14), (20) and (23) can be written using the Laplace transform method and the Green function approach as

$$E(y, t) = \int_C d\omega E(\omega, y) \exp(-i\omega t), \quad (24)$$

where [11]

$$E(\omega, y) = \frac{1}{W(\omega)} \left[ E_1(\omega, y) \int_{-\infty}^y d\bar{y} F(\omega, \bar{y}) E_2(\omega, \bar{y}) + E_2(\omega, y) \int_y^{+\infty} d\bar{y} F(\omega, \bar{y}) E_1(\omega, \bar{y}) \right]. \quad (25)$$

Here,  $E_1(\omega, y)$  and  $E_2(\omega, y)$  are independent solutions of Eqs. (20) and (23) satisfying the open boundary conditions  $E_1(\omega, y) = \exp(ik_{\perp}y)$  for  $y \rightarrow \infty$  and  $E_2(\omega, y) = \exp(-ik_{\perp}y)$  for  $y \rightarrow -\infty$ , where  $k_{\perp} = \sqrt{\omega^2/c^2 - k_{pe}^2 - k_z^2}$  and the double-valued square-root function is defined as  $\sqrt{a^2 + i0} = |a|$  for any real  $a$ . In addition, the function  $F(\omega, y)$  is related to the initial condition for  $E(y, t = 0)$  and its derivatives. The function  $W(\omega)$  is defined as

$$W(\omega) \equiv \epsilon(\omega, y) [E_1(\omega, y)E_2'(\omega, y) - E_2(\omega, y)E_1'(\omega, y)], \quad (26)$$

and is independent of  $y$ . The expression inside the bracket in Eq. (26) is the Wronskian [11]. Since  $1/(\omega - k_z v_{e0})$  has a continuous derivative for all  $y$ , the function  $\epsilon(\omega, y)$  is the same for both Eq. (20) and Eq. (23) and is equal to

$$\epsilon(\omega, y) = \frac{1}{(k_z^2 + k_{pe}^2 - \omega^2/c^2)} \left[ 1 - \frac{\omega_p^2}{(\omega - k_z v_{e0})^2} \right]. \quad (27)$$

The integration in Eq. (24) is performed along a contour  $C$  in the complex  $\omega$ -plane passing above all singularities of  $E(\omega, y)$ . The singularities of  $E(\omega, y)$  determine the long-time behavior of  $E(y, t)$  for  $t \rightarrow \infty$  which can be obtained by deforming the contour  $C$  into the lower half  $\omega$ -plane. Simple zeros of the function  $W(\omega)$  correspond to poles for the integrand in Eq. (24). For every  $y$ , the functions  $E_1(\omega, y)$  and  $E_2(\omega, y)$  as functions of  $\omega$  will also have singularities on the real axis at  $\omega = \omega_c(y)$  everywhere where

$$\epsilon[\omega_c(y), y] = 0. \quad (28)$$

For every  $y$ , the function  $E(\omega, y)$  may also have singularities at the points  $\omega = 0$ ,  $\omega = k_z v_{e0}(y)$  and  $\omega = k_z v_{e0}(y_n^*)$  where  $y_n^*$  are the singular points of the function  $E(y, t = 0)$  and its derivatives in the lower half complex  $y$ -plane. These singularities arise from the poles of function  $F(\omega, y)$  related to the initial conditions for  $E(y, t = 0)$  and its derivatives. Moreover, the points  $\omega = \pm \sqrt{\omega_{pe}^2 + c^2 k_z^2}$  are branch points for function  $E(\omega, y)$ . Using Eqs. (24) and (25), the long-time behavior of  $E(y, t)$  can then be expressed as

$$E(y, t) \approx \sum_{\lambda_i} A_i \exp(-i\omega_i t) E_i(y) + \int_{\sqrt{c^2 k_z^2 + \omega_{pe}^2}}^{\infty} d\bar{\omega} [\exp(-i\bar{\omega} t) A(\bar{\omega}, y) + \exp(i\bar{\omega} t) A(-\bar{\omega}, y)] \quad (29)$$

$$+ B(y) + \exp[-ik_z v_{e0}(y)t] [C_1(y) + D_1(y) \ln(t)] t^{-\alpha_1} + \exp[-i\omega_c(y)t] [C_2(y) + D_2(y) \ln(t)] t^{-\alpha_2},$$

where  $A(\omega, y) \equiv E(\omega + i\delta, y) - E(\omega - i\delta, y)$  with  $\delta \rightarrow 0_+$ . The constants  $A_i$  appearing in the first sum in Eq. (29) and the functions  $B(y)$ ,  $C_i(y)$ ,  $D_i(y)$  ( $i = 1, 2$ ) are determined from the initial conditions. The power exponents  $\alpha_1$  and  $\alpha_2$  depend on the type of singularities at  $\omega = k_z v_{e0}(y)$  and  $\omega = \omega_c(y)$  respectively. In Eq. (29),  $\omega_i$  are simple zeros of the function  $W(\omega)$ , and we have used the fact that if  $W(\omega_i) = 0$  then  $E_1(\omega_i, y) = CE_2(\omega_i, y)$ , where  $C$  is a non-zero constant. For such  $\omega = \omega_i$ , Eqs. (20) and (23) can be viewed as eigenvalue equations, which together with the dispersion relation  $W(\omega_i) = 0$  determine the eigenfunction  $E_i(y) = E_1(\omega_i, y) = CE_2(\omega_i, y)$  which corresponds to the eigenvalue  $\omega_i$ .

Since the the perturbation described by Eqs. (20) and (23) is electromagnetic in nature, the long-time behavior is the sum of two parts. First is the unlocalized part which is radiated away [the integral in Eq. (29) with frequencies  $\omega^2 > \omega_{pe}^2 + c^2 k_z^2$ ]. The second is the localized part which is the part of the perturbation localized near the beam edge by the background electron flow velocity neutralizing the ion beam current. This second part consists of the continuous spectra contribution [last three terms in Eq. (29)], and the discrete spectra contribution (the first sum) with the discrete spectra determined from the equation  $W(\omega) = 0$ , where the function  $W(\omega)$  is given by Eq. (26).

In the following analysis we neglect the effects of the discontinuity in the density profile of the background electrons ( $\omega_{pe}^2$  and  $k_{pe}^2$ ) across the beam edge at  $y = 0$ . These effects contribute corrections of order  $n_b/n_{e0} \ll 1$  to the mode frequencies, and can be neglected. With this approximation in mind, Eqs. (20) and (23) can be expressed as

$$\frac{d^2}{dy^2} E - b \frac{d^2}{dy^2} (bE) = -k_{\perp}^2 (1 - b^2) E, \quad \omega_{ce} \neq 0, \quad (30)$$

$$\frac{d^2}{dy^2} E - \frac{d}{dy} b^2 \frac{d}{dy} E = -k_{\perp}^2 (1 - b^2) E, \quad \omega_{ce} = 0, \quad (31)$$

where  $E \equiv E_z$ ,  $b = \omega_{pe}/[\omega - k_z v_{e0}(y)]$ , and  $k_{\perp}^2 = -k_z^2 - \omega_{pe}^2/c^2 + \omega^2/c^2$ .

It follows from Eq. (29) that the function  $E(y, t)$  will grow exponentially, or that instability exists as  $t \rightarrow \infty$ , provided there are eigenvalues  $\omega_i$  satisfying the dispersion relation  $W(\omega_i) = 0$  with  $Im\omega_i > 0$ . In what follows we will show that the correct eigenvalue equation (30) has no eigenvalues with  $Im\omega_i > 0$ , and therefore the system is stable. On the other hand, the incorrect eigenvalue equation (31) possesses unstable eigenvalues with  $Im\omega_i > 0$ . The eigenfunctions  $E_i(y)$  corresponding to eigenvalues  $\omega_i$  are localized near the beam edge and therefore satisfy the boundary conditions  $E \rightarrow 0$  as  $y \rightarrow -\infty$  or  $y \rightarrow +\infty$ , which requires  $Imk_{\perp} > 0$ . Note that two-stream instability requires  $\omega \sim k_z v_{e0}$ , and therefore we can neglect the term  $\omega^2/c^2 \sim (v_{e0}/c)^2 k_z^2 \ll k_z^2$  in Eqs. (30) and (31). In what follows we consider only modes with  $|\omega^2| \ll \omega_{pe}^2 + c^2 k_z^2$ . In this case, we approximate  $-k_{\perp}^2 \approx k_z^2 + \omega_{pe}^2/c^2$  in Eqs. (30) and (31).

Because the function  $W(\omega)$  is independent of  $y$ , in what follows we evaluate it at  $y = 0$ .

$$W(\omega) = [1 - b^2(0)][E_1'(0)E_2(0) - E_2'(0)E_1(0)]. \quad (32)$$

This is convenient, because the point  $y = 0$  is a symmetry point for the flow velocity profile  $v_{e0}(y)$ . We need to find solutions  $E_1(y)$  for  $y > 0$  behaving as  $\exp(-|k_\perp|y)$  as  $y \rightarrow +\infty$ , and  $E_2(y)$  for  $y < 0$  behaving as  $\exp(|k_\perp|y)$  as  $y \rightarrow -\infty$ . Introducing variable  $s = \exp(-y/\delta_{pe})$  for  $y > 0$ , and  $s = \exp(y/\delta_{pe})$  for  $y < 0$ , the equation for  $E$  can be expressed as

$$(p-s)^2[(p-s)^2 - q^2]s\psi'' + \psi'[(1+2a)(p-s)^2((p-s)^2 - q^2) + 2q^2s(s-p)] \\ + q^2\psi[2a(s-p) - m(s+p)] = 0, \quad (33)$$

where  $E = s^a\psi(s)$ ,  $a = |k_\perp|\delta_{pe} = (1 + k_z^2\delta_{pe}^2)^{1/2}$ , and  $q = 2\omega_{pe}/|k_z|v_{e0}^{max} = 2/(\beta_{e0}|k_z|\delta_{pe})$ . Here,  $\beta_{e0} \equiv v_{e0}^{max}/c$ . Since the functions  $E$  are determined up to a multiplicative constant, we can impose the boundary condition  $\psi(0) = 1$ . Here  $p = p_+ \equiv 1 + 2\lambda$  for  $y > 0$ , and  $p = p_- \equiv 1 - 2\lambda$  for  $y < 0$ , and  $\omega = k_z v_{e0}^{max}(1/2 - \lambda)$ . Moreover,  $m = 1$  corresponds to Eq. (30), and  $m = 0$  corresponds to Eq. (31). Taking the limit  $s \rightarrow 0$  ( $|y| \rightarrow \infty$ ) in this equation, we obtain the second boundary condition for the derivative of  $\psi$ , which can be expressed as

$$\psi'(0) = \frac{1}{p} \frac{m + 2a}{(1 + 2a)} \frac{q^2}{(p^2 - q^2)}. \quad (34)$$

The function  $W(\omega)$  can be written as

$$W(\lambda) \equiv \left(1 - \frac{q^2}{4\lambda^2}\right) [2a\psi_+(1)\psi_-(1) + \psi'_+(1)\psi_-(1) + \psi'_-(1)\psi_+(1)], \quad (35)$$

where  $\psi_+$  denotes the solution of Eq. (33) with  $p = p_+ \equiv 1 + 2\lambda$ , and  $\psi_-$  denotes the solution of Eq. (33) with  $p = p_- \equiv 1 - 2\lambda$ . Note that the function  $W(\lambda)$  is an even function of  $\lambda$  with  $W(\lambda) = W(-\lambda)$ . It also satisfies the relation  $W^*(\lambda) = W(\lambda^*)$ , where  $*$  denotes complex conjugate.

Before showing the numerical solution to the dispersion relation  $W(\lambda) = 0$ , we analyze Eq. (33) analytically for the case of perturbations with  $q \gg 1$  and  $\lambda \sim 1$ . In the case  $q \gg 1$ , and arbitrary  $a$  satisfying  $a^2 = 1 + 4/(\beta_{e0}^2 q^2)$ , Eq. (33) becomes

$$(p-s)^2s\psi'' + \psi'[(1+2a)(p-s)^2 + 2s(p-s)] \\ + \psi[2a(p-s) + m(s+p)] = 0. \quad (36)$$

For the case of zero self-magnetic field ( $m = 0$ ) the solution of this equation satisfying the boundary condition  $\psi(0) = 1$  is given by

$$\psi = {}_2F_1 \left[ \mu(a), \eta(a), \gamma(a), \frac{s}{p} \right]. \quad (37)$$

Here  ${}_2F_1$  is the hypergeometric function [12], where  $\mu(a) = a - 1 + \sqrt{1 + a^2}$ ,  $\eta(a) = a - 1 - \sqrt{1 + a^2}$ , and  $\gamma(a) = 1 + 2a$ . The dispersion relation can be expressed as

$$-\frac{W(\lambda, a)}{q^2} = \frac{1}{4\lambda^2} \left( {}_2F_1 \left[ \mu, \eta, \gamma, \frac{1}{p_+} \right] \left\{ \gamma {}_2F_1 \left[ \mu, \eta, \gamma, \frac{1}{p_-} \right] - \left( \frac{2}{p_-} \right) {}_2F_1 \left[ \mu + 1, \eta + 1, \gamma + 1, \frac{1}{p_-} \right] \right\} \right. \\ \left. + {}_2F_1 \left[ \mu, \eta, \gamma, \frac{1}{p_-} \right] \left\{ \gamma {}_2F_1 \left[ \mu, \eta, \gamma, \frac{1}{p_+} \right] - \left( \frac{2}{p_+} \right) {}_2F_1 \left[ \mu + 1, \eta + 1, \gamma + 1, \frac{1}{p_+} \right] \right\} \right) = 0, \quad (38)$$

where  $p_+ = 1 + 2\lambda$ , and  $p_- = 1 - 2\lambda$ . The unstable solution to Eq. (38) is purely imaginary  $\lambda = i|\lambda|$  and is plotted in Fig. 3 as a function of  $a = (k_z^2 \delta_{pe}^2 + 1)^{1/2}$ . The unstable complex oscillation frequency is given by  $\omega = k_z v_{e0}^{max} / 2 + i |k_z| v_{e0}^{max} |\lambda|$ .

For  $\lambda \ll 1$ , the approximate solution to Eq. (38) can be obtained by expanding the function  $W(\lambda, a)$  near  $\lambda = 0$ , and is given by

$$\lambda = \frac{i}{2a} \exp(-a - 2\gamma), \quad (39)$$

where  $\gamma = 0.577216..$  is the Euler constant. It follows from Eq. (39) that the growth rate is reduced according to the exponential factor

$$Im\omega \approx 0.16 \left( \frac{v_{e0}^{max}}{c} \right) \omega_{pe} \exp(-|k_z| \delta_{pe}), \quad (40)$$

for short-wavelength perturbations with  $k_z^2 \delta_{pe}^2 \gg 1$ .

For the case of non-zero self-magnetic field ( $m = 1$ ), the solution to Eq. (36) satisfying the boundary condition  $\psi(0) = 1$  is given by

$$\psi = 1 - \frac{s}{p}. \quad (41)$$

The corresponding dispersion relation can be written as

$$\frac{W(\lambda, a)}{q^2} = \frac{-1}{4\lambda^2 p_+ p_-} \{ (p_+ - 1)[a(p_- - 1) - 1] + (p_- - 1)[a(p_+ - 1) - 1] \} = \frac{2a}{1 - 4\lambda^2} = 0. \quad (42)$$

This equation has no solutions. Therefore, we conclude that in the limit  $q^2 = (2\omega_p / k_z v_{e0}^{max})^2 \gg 1$ , the magnetic field in the current layer completely stabilizes the instability.

Now let us consider the opposite limit with  $q^2 \lesssim 1$ . In this limit,  $a \gg 1$  and Eq. (33) reduces to

$$\psi'(p - s)[(p - s)^2 - q^2] - q^2 \psi = 0. \quad (43)$$

The solution satisfying the boundary condition  $\psi(0) = 1$  is given by

$$\psi = \left[ \frac{1 - q^2/p^2}{1 - q^2/(p - s)^2} \right]^{1/2} + O(1/a). \quad (44)$$

The function  $W(\lambda)$  in Eq. (35) can be expressed as

$$\begin{aligned} W &= 2a [(1 - q^2/p_+^2)(1 - q^2/p_-^2)]^{1/2} + O(1) \\ &= 2a \frac{[(1 + q)^2 - 4\lambda^2]^{1/2} [(1 - q)^2 - 4\lambda^2]^{1/2}}{1 - 4\lambda^2}, \end{aligned} \quad (45)$$

which has only the real zeros  $\lambda^2 = (1 \pm q)^2/4$ . Therefore, in this limit, both Eqs. (30) and (31) have no growing solutions. The limit  $a \gg 1$  corresponds to the case of strongly localized perturbations. Note, that in the limit,  $q^2 \gg 1$  and  $\lambda \sim 1$ , Eq. (45) reduces to Eq. (42). The function  $W(\lambda)$  in Eq. (45) has branch points at  $\lambda = \pm(1 \pm q)/2$ . Therefore, the function  $W(\lambda)$  is analytic everywhere in the complex  $\lambda$ -plane, with the cut along the lines connecting  $\lambda = -(1 + q)/2$  and  $\lambda = -(q - 1)/2$ , and the line connecting  $\lambda = (q - 1)/2$  and  $\lambda = (q + 1)/2$  for  $q > 1$ . For  $q < 1$ , the cut extends from  $\lambda = -(1 + q)/2$  to  $\lambda = (q + 1)/2$ . As we already mentioned, these cuts correspond to the continuous spectra of real frequencies, which represent stable local plasma oscillations with frequencies between  $\omega = \pm\omega_{pe} + k_z v_{0e}^{max}$  and  $\omega = \pm\omega_{pe}$ .

For arbitrary values of the parameters  $q$  and  $a$ , we evaluate the value of the function  $W(\lambda)[1 - 4\lambda^2]$  by solving Eq. (36) numerically for the case with  $m = 1$ . Here we multiplied the function in Eq. (35) by the factor  $[1 - 4\lambda^2]$  to remove common poles at  $\lambda = \pm 1/2$ .

Figures Fig. 4-6 show contour plots of the zeros of the real and imaginary parts of the function  $W(\lambda)[1 - 4\lambda^2]$  for  $\beta = 0.25$  for several characteristic values of the parameter  $q$ . In the range  $q < 1$ , we chose  $q = 0.6$  ( $a = 13.37$ ) in Fig. 4. For the range  $1 < q < 2$ , we chose  $q = 1.6$  ( $a = 5.1$ ) in Fig. 5. For the range  $q > 2$ , we chose  $q = 3$  ( $a = 2.85$ ) in Fig. 6. Here, we only present the plots in the first quadrant where  $Re\lambda > 0, Im\lambda > 0$ . The value of the function in the entire plane can be recovered using the symmetry relations,  $W(\lambda) = W(-\lambda)$  and  $W(\lambda^*) = W^*(\lambda)$ , where  $*$  denotes complex conjugate.

The analytical properties of the function  $W(\lambda)$  for arbitrary values of  $q$  are quite similar to the function in Eq. (45). For all values of the parameter  $q$ , the function  $W(\lambda)[1 - 4\lambda^2]$  as a function of complex argument  $\lambda$  is zero only at  $\lambda = \pm(1 \pm q)/2$ , where it also has branch points. For  $q > 1$ , the quantity  $Im\{W(\lambda)[1 - 4\lambda^2]\}$  has a jump across the line connecting  $\lambda = -(1 + q)/2$  and  $\lambda = -(q - 1)/2$ , and the line connecting  $\lambda = (q - 1)/2$  and  $\lambda = (q + 1)/2$ . Therefore, the function  $W(\lambda)[1 - 4\lambda^2]$  is analytic everywhere in the complex  $\lambda$ -plane, with the cut along these lines. For  $q < 1$ , the cut extends from  $\lambda = -(1 + q)/2$  to  $\lambda = (q + 1)/2$ .

## V. CONCLUSIONS

In conclusion, we have considered in detail the stability properties of the return-current layer for an intense nonrelativistic heavy ion beam with sharp-edge density profile propagating through collisionless neutralizing plasma. Unlike all previous analyses [8–10] which assumed (unrealistically) complete beam current neutralization, we have considered the stability properties of the current layer self-consistently generated by the ion beam propagating through the background plasma. The current layer has a finite width  $\delta_{\perp} = c/\omega_{pe}$ , and a finite self-magnetic field  $\omega_{ce} \sim (Z_b n_b/n_0)(v_b/c)\omega_{pe}$  [see Eq. (11)], where  $\omega_{ce}$  is the electron cyclotron frequency. To quantify the importance of the finite layer width and the layer self-magnetic field, we compared detailed stability properties of the layer with and without the effects of the self-magnetic field. As we have shown, the finite width of the layer reduces the growth rates of the unstable modes for  $k_z^2 \omega_{pe}^2/c^2 \gg 1$  according to  $Im\omega \sim (Z_b n_b/n_0)(v_b/c)\omega_{pe} \exp(-|k_z|\omega_{pe}/c)$  [see Eq. (39)], but does not eliminate the instability. Because the residual maximum growth rate is of order the electron cyclotron frequency in the layer, the mode frequency is strongly affected by the layer self-magnetic field. The detailed analysis of the dispersion function  $W(\omega)$  in Sec. IV has shown that the mode corresponding to the fast two-stream instability is completely eliminated if the effects of both the finite layer width and self-magnetic field are taken into account.

Our results have important significance for the design of systems employing background plasma to neutralize the space charge of intense ion beams, e.g., for recent designs of the beam-plasma section for the final longitudinal and transverse focusing of heavy ion beams for high energy density physics applications [1–4]. Since the fast electron-electron two-stream mode is eliminated, the remaining two-stream instabilities are between the plasma electrons and beam ions [8] or the plasma electrons and the plasma ions [8]. As recent analyses have shown, the growth rate of these instabilities can be significantly reduced by imposing a longitudinal velocity tilt on the ion beam needed to compress the beam longitudinally [13–15]. On the other hand as the ion beam is compressed transversely, the growth rate of the two-stream instability between the plasma electrons and the beam ions increases due to the increase in density of the neutralizing electrons [16, 17].

### Acknowledgements

This research was supported by the U. S. Department of Energy. It is a pleasure to acknowledge

- [1] P. K. Roy, S. S. Yu, E. Henestroza, A. Anders, F. M. Bieniosek, J. Coleman, S. Eylon, W. G. Greenway, M. Leitner, B. G. Logan, W. L. Waldron, D. R. Welch, C. Thoma, A. B. Sefkow, E. P. Gilson, P. C. Efthimion and R. C. Davidson, *Phys. Rev. Lett.* **95**, 234801 (2005).
- [2] B. G. Logan, F. M. Bieniosek, C. M. Celata, J. Coleman, W. Greenway, E. Henestroza, J. W. Kwan and P. K. Roy, *Nucl. Instr. Meth. Phys. Res.* **A 577**, 1 (2007).
- [3] A. B. Sefkow, R. C. Davidson, I. D. Kaganovich, E. P. Gilson, P. K. Roy, P. A. Seidl, S. S. Yu and J. J. Barnard, *Nucl. Instr. Meth. Phys. Res.* **A 577**, 289 (2007).
- [4] D. R. Welch, D. V. Rose, C. Thoma, A. B. Sefkow, I. D. Kaganovich, P. A. Seidl, S. S. Yu and P. K. Roy, *Nucl. Instr. Meth. Phys. Res.* **A 577**, 231 (2007).
- [5] I. D. Kaganovich, A. B. Sefkow, E. A. Startsev, R. C. Davidson and D. R. Welch, *Nucl. Instr. and Meth. Phys. Res.* **A 577**, 93 (2007).
- [6] I. D. Kaganovich, E. A. Startsev and R. C. Davidson, *Nucl. Instr. and Meth. Phys. Res.* **A 544**, 383 (2005).
- [7] I. D. Kaganovich, G. Shvets, E. A. Startsev and R. C. Davidson, *Phys. Plasmas* **8**, 4180 (2001).
- [8] R. C. Davidson, I. Kaganovich, H. Qin, E. A. Startsev, D. R. Welch, D. V. Rose and H. S. Uhm, *Phys. Rev. ST Accel. Beams* **7**, 114801 (2004); R. C. Davidson et al., *Nucl. Instr. and Meth. Phys. Res.* **A**, in press (2009).
- [9] D.V. Rose, T.C. Genoni, D.R. Welch and C.L. Olson, in *Proceedings of the 2003 Particle Accelerator Conference (Portland, Oregon, 2003)*, pp. 3165-3167.
- [10] D.V. Rose, T.C. Genoni, D.R. Welch and E.P. Lee, *Nucl. Instr. and Meth. Phys. Res.* **A 544**, 389 (2005).
- [11] C. M. Bender and S. A. Orszag, *Advanced Mathematical Methods for Scientists and Engineers* (McGraw-Hill book company, New York, 1978).
- [12] I. S. Gradshteyn and I. M. Ryzhik, *Tables of Integrals, Series, and Products* (Academic Press, New York, 1965).
- [13] E. A. Startsev and R. C. Davidson, *Phys. Plasmas* **13**, 062108, 2006.
- [14] E. A. Startsev and R. C. Davidson, *Nucl. Instr. and Meth. Phys. Res.* **A 577**, 79 (2007).
- [15] D. V. Rose, T. C. Genoni, D. R. Welch, E. A. Startsev and R. C. Davidson, *Phys. Rev. ST Accel. Beams* **10**, 034203 (2007).
- [16] E. A. Startsev, R. C. Davidson and M. Dorf, *Nucl. Instr. and Meth. Phys. Res.* **A**, in press (2009).
- [17] T.C. Genoni, D.V. Rose, D.R. Welch and E.P. Lee, *Phys. Plasmas* **11**, L73 (2004).

## FIGURE CAPTIONS

Fig.1 : 2D planar geometry for ion beam propagation for  $k_{\perp}\delta_{\perp} \gg 1$ . The ion beam propagates in the  $z$ -direction with axial velocity  $v_b$ . The neutralizing background electrons are flowing in the same direction with average axial velocity  $v_{e0}(y)$  which is a function of the transverse coordinate  $y$ . The self-magnetic field  $B_0$  generated by the uncompensated beam current is in the  $x$ -direction.

Fig.2 : Schematic of the current layer near the beam edge ( $y = 0$ ) for an ion beam with number density  $n_b$ . The background electron flow velocity profile  $v_{e0}(y)$  smoothly increases from zero outside the beam to the value  $v_{e0}^{max} = (Z_b n_b / n_{e0}) v_b$  inside the beam over the characteristic length scale  $\delta_{pe} = c / \omega_{pe}$  [see Eq. (10)].

Fig.3 : Normalized growth rate  $Im\omega / (k_z v_{e0}^{max})$  plotted as a function of normalized transverse wavenumber  $a = (1 + c^2 k_z^2 / \omega_{pe}^2)^{1/2}$  as determined from the solution to Eq. (38).

Fig.4 : Contour plots of the zeros of the real (thin line) and imaginary (thick line) parts of the function  $W(\lambda)[1 - 4\lambda^2]$  for  $\beta_{e0} = 0.25$  and  $q = 2\omega_{pe} / |k_z| v_{e0}^{max} = 0.6$  ( $a = 13.37$ ).

Fig.5 : Contour plots of the zeros of the real (thin line) and imaginary (thick line) parts of the function  $W(\lambda)[1 - 4\lambda^2]$  for  $\beta_{e0} = 0.25$  and  $q = 2\omega_{pe} / |k_z| v_{e0}^{max} = 1.6$  ( $a = 5.10$ ).

Fig.6 : Contour plots of the zeros of the real (thin line) and imaginary (thick line) parts of the function  $W(\lambda)[1 - 4\lambda^2]$  for  $\beta_{e0} = 0.25$  and  $q = 2\omega_{pe} / |k_z| v_{e0}^{max} = 3$  ( $a = 2.85$ ).

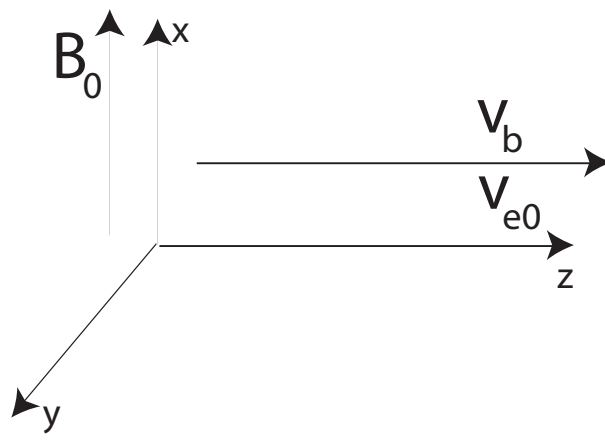


FIG. 1:

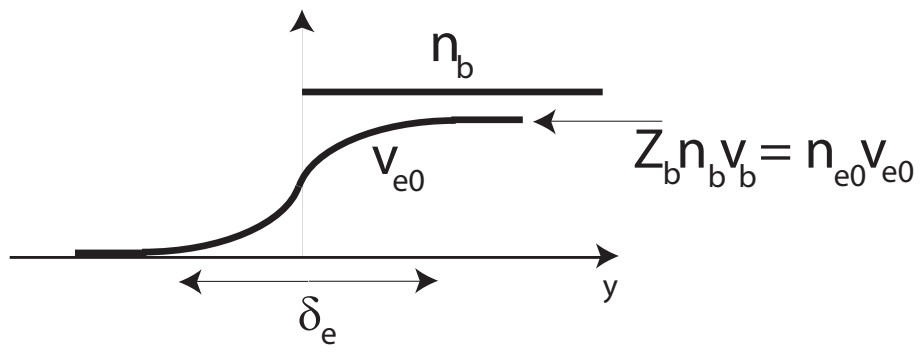


FIG. 2:

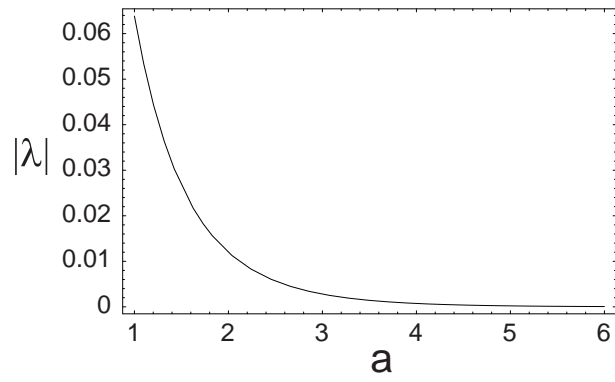


FIG. 3:

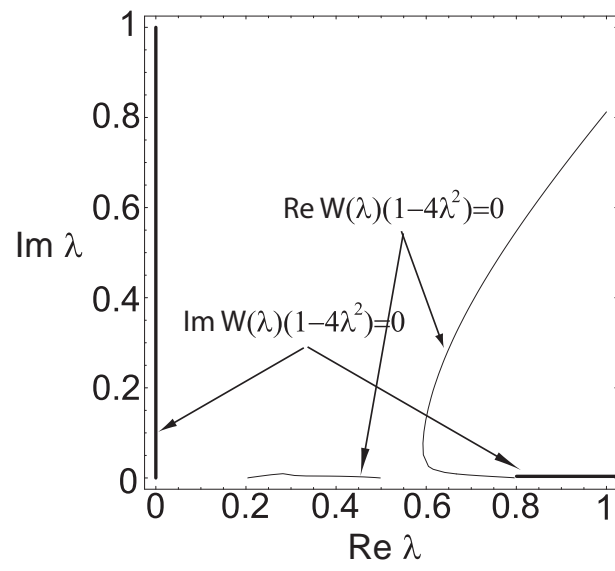


FIG. 4:

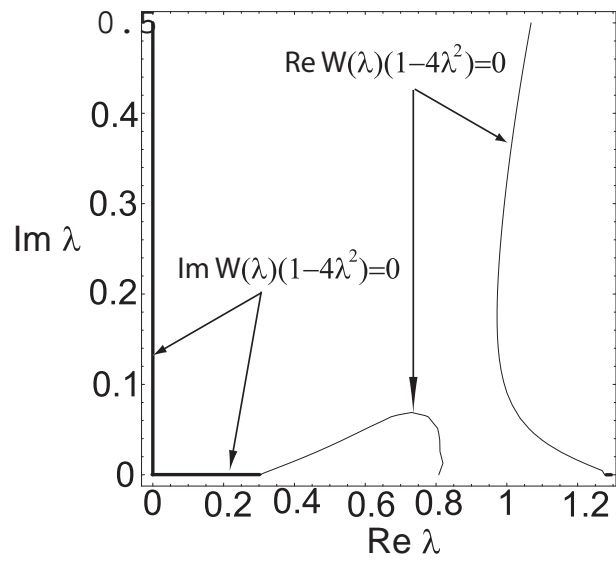


FIG. 5:

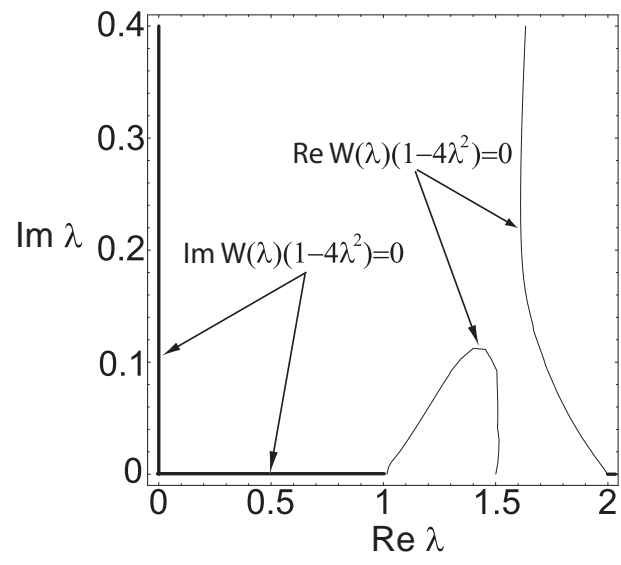


FIG. 6: